Advances in Aircraft and Spacecraft Science, *Vol. 4, No. 4 (2017) 353-369*
DOI: https://doi.org/10.12989/aas.2017.4.4.353

Improving wing aeroelastic characteristics using periodic design

Hossam T. Badran*[1], Mohammad Tawfik[2a] and Hani M. Negm[1b]

[1]*Aerospace Engineering Department, Cairo University, Giza, Egypt*
[2]*Aerospace Engineering, University of Science and Technology, Zewail City for Science and Technology, Giza, Egypt*

(Received August 17, 2016, Revised October 21, 2016, Accepted February 11, 2016)

Abstract. Flutter is a dangerous phenomenon encountered in flexible structures subjected to aerodynamic forces. This includes aircraft, buildings and bridges. Flutter occurs as a result of interactions between aerodynamic, stiffness, and inertia forces on a structure. In an aircraft, as the speed of the flow increases, there may be a point at which the structural damping is insufficient to damp out the motion which is increasing due to aerodynamic energy being added to the structure. This vibration can cause structural failure, and therefore considering flutter characteristics is an essential part of designing an aircraft. Scientists and engineers studied flutter and developed theories and mathematical tools to analyze the phenomenon. Strip theory aerodynamics, beam structural models, unsteady lifting surface methods (e.g., Doublet-Lattice) and finite element models expanded analysis capabilities.

Periodic Structures have been in the focus of research for their useful characteristics and ability to attenuate vibration in frequency bands called "stop-bands". A periodic structure consists of cells which differ in material or geometry. As vibration waves travel along the structure and face the cell boundaries, some waves pass and some are reflected back, which may cause destructive interference with the succeeding waves. This may reduce the vibration level of the structure, and hence improve its dynamic performance.

In this paper, for the first time, we analyze the flutter characteristics of a wing with a periodic change in its sandwich construction. The new technique preserves the external geometry of the wing structure and depends on changing the material of the sandwich core. The periodic analysis and the vibration response characteristics of the model are investigated using a finite element model for the wing. Previous studies investigating the dynamic bending response of a periodic sandwich beam in the absence of flow have shown promising results.

Keywords: vibration; flutter; wing; sandwich beam; finite elements; periodic structure; stop bands

1. Introduction and literature survey

Physical systems such as wings can be modelled as beams, whose study frequently results in partial differential equations which cannot be solved by an exact analytic solution. Two beam

*Corresponding author, Ph.D. Student, E-mail: htbadran@hotmail.com
[a]Associate Professor, E-mail: mohammad.tawfik@gmail.com
[b]Professor, E-mail: hnegm_cu@hotmail.com

http://www.techno-press.org/?journal=aas&subpage=7 ISSN: 2287-528X (Print), 2287-5271 (Online)

fictitious boundary inside the structure. Using the method of static condensation, the internal nodes/degrees of freedom of the substructure can be eliminated, thus reducing the size of the global matrices of the structure. When the set of equations of the substructure can be manipulated to collect the forces and displacements of one end of the substructure on one side of the equation, and relate them to those on the other end with a matrix relation, this matrix relation is called the transfer matrix of the structure. The transfer matrix of a substructure, other than being of reduced order, is then multiplied by that of the neighbouring structure, in contrast with the superposition method that is used in conventional numerical techniques. Thus, the matrix system that describes the dynamics of the structure becomes of significantly smaller size. The transfer matrix method becomes of even more appealing features when the substructures can be selected in a manner that they are all identical, thus, calculating the transfer matrix for one substructure is sufficient to describe the dynamics of the whole structure easily. In this section, we review the research works performed in the area of wave propagation in periodic structures. Ungar (1966) derived an expression that describes the steady state vibration of an infinite beam uniformly supported on impedances. Later, Gupta (1970), presented an analysis for periodically-supported beams that introduced the concepts of the cell and the associated transfer matrix. He presented the propagation and attenuation parameter plots which form the foundation for further studies of one-dimensional periodic structures. Faulkner and Hong (1985), presented a study of general mono-coupled periodic systems. Their study analysed the free vibration of spring-mass systems as well as point-supported beams using analytical and finite element methods. Mead and Yaman (1991), presented a study of the response of one-dimensional periodic structures subject to periodic loading. Their study involved generalization of the support condition to involve rotational and displacement springs as well as impedances. The effects of the excitation point as well as the elastic support characteristics on the pass and stop characteristics of the beam were presented. Langley (1996), presented the basic property of a symplectic matrix whose eigenvalues appear in pairs, one of which is the reciprocal of the other. This property of the transfer matrix introduces simplicity into the analysis; but unfortunately, introduces numerical instabilities in the numerical solution of structures with a large number of cells.

Flutter is defined as a dynamic instability of an elastic structure in a fluid flow, caused by positive feedback between the body's deflection and the forces exerted by the fluid flow. In a linear system, 'flutter point' is the point at which the structure is undergoing simple harmonic motion-zero net damping, and so any further decrease in the net damping will result in a self-oscillation and eventual failure. Georghiades and Banerjee (1997) investigated the flutter behaviour of uniform composite wings using parametric study. The wing is idealized as a bending torsion (materially) coupled composite beam with cantilever end conditions for which the frequency equation and mode shapes in free vibration are presented in closed analytical form. Guo *et al.* (2003), presented an analytical study on optimization of a laminated composite wing structure for achieving a maximum flutter speed and a minimum weight without strength penalty. Attention has been paid mainly to the effect on flutter speed of the bending, torsion and, more importantly, the bending-torsional coupling rigidity, which is usually associated with asymmetric laminate lay-up. Kameyama and Fukunaga (2007), treated the flutter and divergence characteristics of composite plate wings with various sweep angles. The effect of laminate configuration on the flutter and divergence characteristics is investigated for composite plate wings. Guo (2007), presented an investigation into a minimum weight optimal design and aeroelastic tailoring of an aerobatic aircraft wing structure. Based on a minimum weight composite wing box model of adequate strength the investigation was focused on the aeroelastic tailoring of

Table 1 Natural frequencies (Hz) of shear sensory actuated cantilever wing

	1st	2nd	3rd	4th	5th
Finite element Benjeddou *et al.* (1999)	985	3912	8305	17273	25980
Finite element (short circuited)	985	3911	8297	17226	25849
Finite element (open circuited)	988	3924	8352	17406	26273

Then, the strain of different layers and the rotation of core layer due to axial and bending actions are obtained by differentiating the above displacements with respect to (x). The core layer the shear strain and rotation will be described according to Fig. 2 as having these values: $\gamma_{xz}=(u_t-u_b)/h_c+(A_3/h_c)\partial w/\partial x$ and $\theta(x)=(u_t-u_b)/h_c+(A_1/h_c)\partial w/\partial x$ respectively. Where, subscripts (t), (b) and (c) denote top, bottom and core layers respectively. A_i are defined in Appendix 1.

3. Constitutive equations

The three dimensional linear constitutive equations of orthotropic PZT ceramic core of the shear mode have the following form, Trindade *et al.* (1999).

$$\begin{Bmatrix} \sigma_x^c \\ \tau_{zx} \\ D_3 \end{Bmatrix} = \begin{bmatrix} Q_{33} & 0 & 0 \\ 0 & Q_{55} & -e_{15} \\ 0 & e_{15} & \in_1 \end{bmatrix} \begin{Bmatrix} \varepsilon_x^c \\ \gamma_{zx} \\ E_3 \end{Bmatrix} \tag{2}$$

The linear constitutive equations of face layers have the form

$$\{\sigma_k\} = [E_k] \times \{\varepsilon_k\} \tag{3}$$

The linear constitutive equation of the electric potential applied through the core layer has the following form

$$\emptyset_c = \bar{\emptyset}_c + \frac{V_c}{h_c} z \tag{4}$$

The electric potential in the core is shown to be linear in the thickness direction.

Since ($E_3=-\partial\phi_c/\partial z$), so Eq. (4) reduces to

$$E_3 = -\frac{V_c}{h_c} \tag{5}$$

4. Development of equations of motion

The dynamic equations of motion in this investigation are developed using Hamilton's principle, Reddy (2002).

$$\delta\Pi = \int_{t1}^{t2} (\delta T - \delta U + \delta W)\, dt = 0 \tag{6}$$

Where, $\delta\Pi$: Total system energy, δT: Kinetic energy , δU: Strain energy and δW: Work done

The element total mass matrix will be derived according to Eq. (8) as: $\delta T_{to}^{p} = \delta\dot{q}^{T}[M_p]\,\dot{q}$. The mechanical and electrical applied force are introduced according to Eq. (9) giving of the variation of external work. The element stiffness matrices, mass matrix and force vector of the adaptive sandwich wing are given in Appendix 2. By substituting the mass, stiffness and force vector in Eq. (6), the equations of motion can be written as

$$[M]\{\ddot{\delta}_m\} + [K_m]\{\delta_m\} + [K_{me}]\{\delta_e\} = \{F_m\} \tag{10}$$

$$[K_{em}]\{\delta_m\} + [K_e]\{\delta_e\} = \{F_e\} \tag{11}$$

Where: δ_m and δ_e are the global nodal generalized displacement and electrical coordinates respectively. By applying electrical boundary conditions such as short-circuited or open-circuited boundary conditions, the coupled governing equation set can be solved explicitly. For voltage driven electrodes (short circuit) where the electric potential δ_e is specified, Eq. (10) results in

$$[M]\{\ddot{\delta}_m\} + [K_m]\{\delta_m\} = \{F_m\} - [K_{me}^{a}]\{\delta_e\} \tag{12}$$

The second term on the right hand side $[K_{me}^{a}]\,\delta_e$ represents the equivalent PZT ceramic loads. The mechanical displacement can be solved from this equation and consequently substituted in Eq. (11) to calculate the electric charges. It can be observed that for short circuited electrodes where $\{\delta_e\} = 0$, Eq. (12) is identical to those where no PZT ceramic electromechanical coupling exists. Then, one ends up with the eigenvalue problem

$$([K_m] - \omega^2[M])\{\delta_m\} = 0 \tag{13}$$

Eq. (13) shows that the natural frequencies and mode shapes of the short-circuited system are the same as those of non-PZT ceramic system.

For open circuited electrodes, the electric charge is zero ($\{F_e\} = 0$), hence, $\{\delta_e\}$ can be obtained from Eq. (11) as: $\{\delta_e\} = -[K_e]^{-1}[K_{em}]\{\delta_m\}$.

By substituting in Eq. (10), we get

$$[M]\{\ddot{\delta}_m\} + ([K_m] - [K_{me}][K_e]^{-1}[K_{em}])\{\delta_m\} = \{F_m\} \tag{14}$$

We find that PZT ceramic electromechanical coupling increases the overall stiffness of the system if the electrodes are open, because of $[Ke]^{-1}$ is negative. In this case the natural frequencies are greater than the case when the coupling is neglected.

A computer code has been developed to calculate the natural frequency in short and open-circuited cases as shown in Table 1. Table 1 compares the calculated values of the first five natural frequencies of the sandwich cantilever beam with (PZT-Foam) core with the results of Benjeddou (1999). The results validate the correctness of the equations, matrices and computer programs of the suggested three-node sandwich beam finite element model using 3-elements, and show that the accuracies of the two models are almost identical. Also, they show that the natural frequencies improve with open circuited condition by attaining higher values.

6. Periodic analysis

Periodic structures can be modelled like any ordinary structure, however, studying the behaviour of one cell is sufficient to determine the stop and pass bands of the complete structure independent of the number of cells. In the present work, the frequency domain is classified into

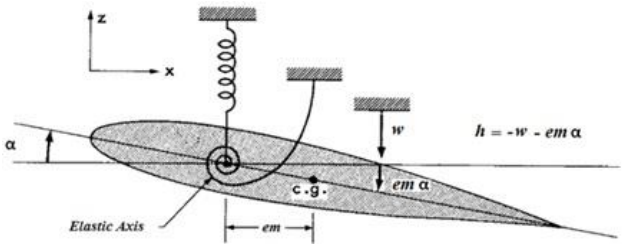

Fig. 4 Two-DOF bending and torsion airfoil model

Where, $\bar{q}$ is the amplitude of the deformation vector, $\bar{F}$ is the amplitude of the load vector, [*M*] is the global mass matrix, and [*K*] is the global stiffness matrix. In Eq. (16) the right hand side is derived using the Aerodynamic model, and the left hand side is derived using the Structural model. The natural frequency (ω) occurs in a free vibration case where the system acts independent of the external forces.

7.1 Structural model

Double symmetry of the structure cross section leads to decoupling of the bending and torsional motions. The loss of cross sectional symmetry leads to a coupling effect between the bending and torsional motions due to an offset between the center of gravity and the shear center; a distance referred to as inertial eccentricity. The resulting equations of motion are inertially coupled, but elastically uncoupled.

The coupled elastic potential energy (U) is given as

$$U = \frac{1}{2}\, EI \int_0^L \left(\frac{\partial^2 w}{\partial y^2}\right)^2 dy + \frac{1}{2}\, GJ \int_0^L \left(\frac{\partial \theta}{\partial y}\right)^2 dy \tag{17}$$

The coupled kinetic energy (*T*) is given as

$$T = \frac{1}{2} \int_{chord} \left(\frac{\partial h}{\partial t}\right)^2 dm \tag{18}$$

By refering to Fig. 4, $h = -w - em\,\alpha$

Substituting (h) in Eq. (18) it can be shown that, Guertin ML (2012)

$$T = \frac{1}{2}\,(\mu) \int_0^L (\dot{w})^2\, dx + \frac{1}{2}\,(2\,S_\alpha) \int_0^L (\dot{w})(\dot{\theta})\, dx + \frac{1}{2}\,(I_\alpha) \int_0^L (\dot{\theta})^2\, dx \tag{19}$$

Where, *EI*: bending rigidity, *GJ*: torsion rigidity, ρ_m: material density, *A*: cross section area, I_o: polar moment of inertia, e_m: inertial eccentricity (offset of center of gravity from the elastic center), μ: mass per unit length $(\rho_m A)$, *b*: half chord , *a*: offset of the mid chord from the elastic axis (non-dimensional), S_a: static mass moment per unit span about the axis $x=ba$, and equals (μe_m), and I_a: mass moment of inertia per unit length, and equals ($\rho_m I_o$). By calculating the potential and kinetic energies of the structural model and applying Hamilton's principle, then using finite elements having two-nodes and three degrees of freedom per node (torsion, transverse displacement and rotation), we get the system of equations representing an eigen value problem. Solving these equations, we get the natural frequencies and mode shapes due to bending and torsion.

Table 2 GOLAND wing frequencies

	Present work	Banerjee (1999)
1st Bending frequency (rad/sec)	49.4922	49.6
1st Torsion frequency (rad/sec)	96.049	97.0

Table 3 GOLAND wing flutter speed (mph)

	No of Elements				Flutter speed (mph)	Reference
	2	3	5	10		
Flutter Speed (mph)	394.93	385.24	380.97	379.32	385.00 Assumed odes	Bisplinghoff *et al.* (1996)

So, the equation of the dynamic system after assembling all matrices can be written as

$$\left(-\omega^2\left[[M]+[A]\right]+[K]\right)\{\bar{q}\}=0 \tag{26}$$

The flutter analysis can be performed using the familiar V−g method, Bisplinghoff *et al.* (1996). The structural damping coefficient (g) is introduced in the equations of motion, representing the amount of damping that must be added to the structure to attain neutral stability at the given velocity. Negative values of structural damping (g) indicate that the structure is stable, while positive values indicate instability. Flutter occurs when the structural damping coefficient (g) equals the actual damping of the structure, which is nearly zero, Hollowell and Dugundji (1984). Substituting in Eq. (26), the following eigenvalue problem is obtained

$$\left([K]^{-1}([M]+[A])-\left(\frac{1+gi}{\omega^2}\right)[I]\right)\{\bar{q}\}=0 \tag{27}$$

The above equation can be solved as

$$\begin{gathered}\left([K]^{-1}\left[[M]+[A]\right]\right)\{\bar{q}\}=\left(\left(\frac{1+gi}{\omega^2}\right)[I]\right)\{\bar{q}\}\\ \left([K]^{-1}\left[[M]+[A]\right]\right)\{\bar{q}\}=(Z[I])\{\bar{q}\}\end{gathered} \tag{28}$$

The above equation can be solved for the complex eigenvalues (Z) for several values of the reduced frequency by equating both the imaginary and real parts on both sides. Then we can calculate the flutter frequency (ω_f), damping (g) and flutter speed (U_f) as follows

$$\omega_f=\sqrt{\frac{1}{Z(Re)}}\ ,\eta=\frac{Z(Im)}{Z(Re)}\ ,\ U_f=\frac{\omega_f\, b}{k} \tag{29}$$

The values of (g) and (ω) are plotted vs. (U_f), and the ω value at g=0 represents the flutter frequency (ω_f). A computer code was developed for the smart periodic wing. The finite element model consists of two models: a structural model, which is a geometric model of the wing, and an aerodynamic model, which calculates the unsteady aerodynamic loads acting on the wing.

7.3 Flutter numerical validation

The Goland wing is a low-aspect-ratio prismatic metallic wing,which has been extensively used for validation in the literature. It is a structurally uncoupled wing with some inertial coupling. The

8.2 Flutter speed of solid core wing

It has been found by applying the proposed model that the flutter speed of the solid core wing at an altitude of 1000 m is 47.5 m/sec.

8.3 Flutter speed of wing with periodic core

The proposed periodic core is a sandwich wing with three layers: the top and bottom layers are made of Aluminium, and the core is periodic PZT Ceramic-Foam side by side. We choose the main geometry of the periodic model to be similar to the solid model, with the same total thickness and total length of the wing. In this case the mass is 458.4 Kg compared to 399.6 Kg for the solid blade. So we will change the thickness of the layers to have a thickness ratio (h_p/h_t) of 0.5 and the lengths of the cells to have a cell length ratio (L_p/L_t) of 0.5. These values reduce the mass of the proposed periodic core model to that of the solid model.

The flutter speed of the sandwich wing has been calculated at the same altitude using the proposed model for 6 pairs of periodic cells. The results show that the flutter speed has increased to 51.53 m/sec, which represents an improvement of 8.5%.

9. Conclusions

Aeroelastic performance of aircraft wing structures is of extreme importance. An aircraft wing must not experience flutter instability at all possible speeds. Periodic design of structures has proved to be useful in improving the dynamic performance in the absence of flow. A periodic structure is composed of repeated groups of cells of different material or geometry. This causes destructive interference between the waves travelling along the structures, and hence reduces its vibration level.

In this paper a periodic wing design is suggested as a beam composed of a core sandwiched between two aluminium faces layers. The beam is divided into cells in which the core is made of piezo ceramic or foam patches in an alternate order. The flutter speed is calculated for such a periodic sandwich wing using finite element method in the structural analysis, and Theodorsen's 2-D thin aerofoil theory with a lift deficiency function for the unsteady aerodynamic analysis, assuming incompressible flow conditions. The wing flutter speed is calculated using V-g method for 6 pairs of periodic cells, and compared with that of the nonperiodic solid wing having the same mass. Results of the calculations show that the flutter speed of the periodic wing is higher than that of the nonperiodic wing having the same mass.

References

Abramovich, H. (1998), "Deflection control of laminated composite beam with piezoceramic layers-closed form solutions", *Compos. Struct.*, **43**(3), 217-231.

Aldraihem, O.J. and Khdeir, A.A. (2000), "Smart beams with extension and thickness-shear piezoelectric actuators", *Smart Mater. Struct.*, **9**(1), 1-9.

Aldraihem, O.J., Wetherhold, R.C. and Singh, T. (1997), "Distributed control of laminated beams: Timoshenko vs. Euler-Bernoulli theory", *J. Intell. Mater. Syst. Struct.*, **8**(2), 149-157.

Badran, H.T. (2008a), "Vibration attenuation of periodic sandwich beams", M.S. Dissertation, Cairo

Thomas, J. and Abbas, B.A. (1975), "Finite element methods for dynamic analysis of Timoshenko beam", *J. Sound Vibr*., **41**, 291-299.

Trindade, M.A., Benjeddou, A. and Ohayon, R. (1999), "Parametric analysis of the vibration control of sandwich beams through shear-based piezoelectric actuation", *J. Intell. Mater. Syst. Struct.*, **10**(5), 377-385.

Ungar, E.E. (1966), "Steady-state response of one-dimensional periodic flexural systems", *J. Acoust. Soc. Am*., **39**(5), 887-894.

Zhang, X. and Sun, C. (1996), "Formulation of an adaptive sandwich beam", *Smart Mater. Struct*., **5**(6), 814-823.

EC

Appendix 1

$B_1=\left(\frac{Q_{33}^c I_c}{h_c^2}+\frac{Q_{33}^c A_c}{4}+Q_{11}^t A_t\right)$,
$B_2=\left(\frac{Q_{33}^c I_c}{h_c^2}+\frac{Q_{33}^c A_c}{4}+Q_{11}^b A_b\right)$
$B_3=\left(\frac{Q_{33}^c I_c (A1)^2}{h_c^2}+\frac{Q_{33}^c A_c (A2)^2}{4}+Q_{11}^t I_t+Q_{11}^b I_b\right)$
$B_4=\left(\frac{Q_{33}^c (A_c)}{4}-\frac{Q_{33}^c I_c}{h_c^2}\right)$,
$B_5=\left(\frac{Q_{33}^c (A_c)(A2)}{4}+\frac{Q_{33}^c I_c (A1)}{h_c^2}\right)$
$B_6=\left(\frac{Q_{33}^c A_c\, A2}{4}-\frac{Q_{33}^c I_c\, A1}{h_c^2}\right)$, $B7=\left(\frac{K_s Q_{55} A_c}{h_c^2}\right)$
$B_8=\left(\frac{K_s Q_{55} A_c (A3)^2}{h_c^2}\right)$, $B9=\left(\frac{K_s Q_{55} A_c}{h_c^2}\right)$
$B_{10}=\left(\frac{K_s Q_{55} A_c (A3)}{h_c^2}\right)$, $B11=\left(\frac{e_{15} A_c}{h_c^2}\right)$
$B_{12}=\left(\frac{e_{15} A_c (A3)}{h_c^2}\right)$, $B13=\left(\frac{\in_1 A_c}{h_c^2}\right)$
$C_1=\left(\frac{E_f I_f}{h_c^2}+\frac{E_f A_f}{4}+Q_{11}^t A_t\right)$
$C_2=\left(\frac{E_f I_f}{h_c^2}+\frac{E_f A_f}{4}+Q_{11}^b A_b\right)$
$C_3=\left(\frac{E_f I_f (A1)^2}{h_c^2}+\frac{E_f A_f (A2)^2}{4}+Q_{11}^t I_t+Q_{11}^b I_b\right)$
$C_4=\left(\frac{E_f A_f}{4}-\frac{E_f I_f}{h_c^2}\right)$,
$C_5=\left(\frac{E_f A_f (A2)}{4}+\frac{E_f I_f (A1)}{h_c^2}\right)$,
$C_6=\left(\frac{E_f A_f (A1)}{4}-\frac{E_f I_{f\,(A2)}}{h_c^2}\right)$,
$C_7=\left(\frac{K_s G_f A_f}{h_c^2}\right)$,
$C_8=\left(\frac{K_s G_f A_f (A3)^2}{h_c^2}\right)$,
$C_9=\left(\frac{K_s G_f A_f}{h_c^2}\right)$, and
$C_{10}=\left(\frac{K_s G_f A_f (A3)}{h_c^2}\right)$.

$D_1=\left(\frac{\rho_c A_c}{4}+\frac{\rho_c I_c}{h_c^2}+\rho_t A_t\right)$,
$D_2=\left(\frac{\rho_c A_c}{4}+\frac{\rho_c I_c}{h_c^2}+\rho_b A_b\right)$,
$D_3=\left(\frac{\rho_c A_c (A2)^2}{4}+\frac{\rho_c I_c (A1)^2}{h_c^2}+\rho_t I_t+\rho_b I_b\right)$,
$D_4=\left(\frac{\rho_c A_c}{4}-\frac{\rho_c I_c}{h_c^2}\right)$,
$D_5=\left(\frac{\rho_c A_c (A2)}{4}+\frac{\rho_c I_c (A1)}{h_c^2}\right)$,
$D_6=\left(\frac{\rho_c A_c (A2)}{4}-\frac{\rho_c I_c (A1)}{h_c^2}\right)$
$D_7=(\rho_t A_t+\rho_c A_c+\rho_b A_b)$
$H_1=\left(\frac{\rho_f A_f}{4}+\frac{\rho_f I_f}{h_f^2}+\rho_t A_t\right)$,
$H_2=\left(\frac{\rho_f A_f}{4}+\frac{\rho_f I_f}{h_f^2}+\rho_b A_b\right)$
$H_3=\left(\frac{\rho_f A_f (A2)^2}{4}+\frac{\rho_f I_f (A1)^2}{h_f^2}+\rho_t I_t+\rho_b I_b\right)$
$H_4=\left(\frac{\rho_f A_f}{4}-\frac{\rho_f I_f}{h_f^2}\right)$,
$H_5=\left(\frac{\rho_f A_f (A2)}{4}+\frac{\rho_f I_f (A1)}{h_f^2}\right)$
$H_6=\left(\frac{\rho_f A_f (A2)}{4}-\frac{\rho_f I_f (A1)}{h_f^2}\right)$
$H_7=\left(\rho_t A_t+\rho_f A_f+\rho_b A_b\right)$

$Q_{33}^c=c_{33}-c_{13}^2/c_{11}$
$Q_{55}=c_{55}$
$A_1=(h_t+h_b)/2$,
$A_2=(h_t-h_b)/2$
$A_3=(h_t+2h_c+h_b)/2$,

■̇ : denotes first derivative with respect to time (t) i.e., time derivative ($\partial/\partial t$)
■′: denotes first derivative with respect to x i.e., spatial derivative
■″: denotes second derivative with respect to (x).

Appendix 2

$$[K_m] = \int_0^L [(N_t')B1(N_t') + (N_b')B2(N_b') + (N_W'')B3\,(N_W'') - (N_t')B4(N_b') - (N_b')\,B4(N_t') + (N_t')B5\,(N_W'') + (N_W'')B5(N_t') + (N_b')B6\,(N_W'') + (N_W'')B6(N_b') + N_tB7\,N_t + N_bB7\,N_b + (N_W')B8\,(N_W') + (N_t)B9\,N_b + N_bB9\,N_t - N_bB10\,(N_W') - (N_W')B10\,N_b + N_tB10\,(N_W') + (N_W')B10\,N_t]\,dx$$

$$[K_{me}^a] = \int_0^L [(N_t)B11(V_c) - (N_b)\,B11(V_c) + (N_W')B12\,(V_c)]\,dx$$

$$[K_{em}^a] = \int_0^L (V_c)B11\,(N_t) - (V_c)B11\,(N_b) + (V_c)B12\,(N_W')\,dx$$

$$[K_e^a] = -\int_0^L (V_c)B13\,(V_c)\,dx$$